Nitric Oxide Binding and Crystallization of Recombinant Nitrophorin I, a Nitric Oxide Transport Protein from the Blood-Sucking Bug *Rhodnius prolixus*†

John F. Andersen,‡ Donald E. Champagne,§ Andrzej Weichsel,‡ José M. C. Ribeiro,|| Celia A. Balfour,‡ Virginia Dress,‡ and William R. Montfort*,‡

Departments of Biochemistry, Veterinary Sciences, and Entomology, University of Arizona, Tucson, Arizona 85721

Received November 21, 1996⊗

ABSTRACT: A nitric oxide transport protein (nitrophorin I) from the salivary glands of the blood-sucking bug *Rhodnius prolixus* has been expressed as an insoluble form in *Escherichia coli*, reconstituted with heme, and characterized with respect to NO binding kinetics and equilibria. NO binding and absorption spectra for recombinant nitrophorin I were indistinguishable from those of the insect-derived protein. The degree of NO binding, the rate of NO release, and the Soret absorption maxima for nitrophorin I were all pH dependent. The NO dissociation constant rose 9-fold over the pH range 5.0−8.3 , from 0.19 $\times 10^{-6}$ to 1.71 $\times 10^{-6}$. The NO dissociation rate rose 2500-fold between pH 5.0 and pH 8.3, from 1.2 $\times 10^{-3}$ to 3.0 s^{-1}. Thus, the NO association rate must also be pH dependent and reduced at pH 5.0 by ∼280-fold. These factors are consistent with nitrophorin function: NO storage in the apparent low pH of insect salivary glands and NO release into the tissue of the insect's host, where vasodilation is induced. The reversible nature of NO binding, which does not occur with most other heme proteins, and the apparent kinetic control of NO release are discussed. We also report crystals of nitrophorin I that are suitable for structure determination by X-ray crystallography. The most promising crystal form contains two protein molecules in the asymmetric unit and diffracts beyond 2.0 Å resolution.

Nitric oxide (NO)[1] is a messenger molecule that has been implicated in an amazingly diverse array of physiological processes. NO is involved in neurotransmission, cell-mediated immune response, muscle relaxation, and vasodilation, and probably affects the functioning of most mammalian cells [reviewed in Bredt and Snyder (1994) and Schmidt and Walter (1994)]. This toxic, gaseous substance acts in many cases by interacting with heme proteins such as guanylate cyclase and prostaglandin H synthase. NO binds to ferrous [Fe(II)] heme proteins with very high affinity, but unlike carbon monoxide it also binds reasonably well to ferric [Fe(III)] heme. In the case of soluble guanylate cyclase, the interaction of NO with the ferrous enzyme is thought to induce an activating conformational change in the protein (Traylor & Sharma, 1992; Tsai, 1994; Stone & Marletta, 1996).

Saliva of the blood-feeding insect *Rhodnius prolixus* contains heme proteins whose function appears to be the transport of nitric oxide into the host skin. Following NO release, vasodilation facilitates feeding. Four separate heme proteins have been isolated from the salivary glands of these insects, and their cDNA sequences have been determined (Champagne et al., 1995; D. Champagne, unpublished data). Together, these related proteins have been given the name nitrophorins I−IV, and their sequences show no significant similarity to any other known proteins, including the globins (D. Champagne, unpublished data). An apparently unrelated (by sequence similarity) protein with similar properties has been isolated from the salivary glands of the bedbug *Cimex lectularius* (Valenzuela et al., 1995).

Nitrophorins exist in the ferric state *in vivo* and display a pH-dependent variable affinity for binding of NO. Binding is slowly reversible at pH 5.0 and freely reversible at pH 8.0 (Ribeiro et al., 1993). The pH dependence appears to be due to a single ionizable group with a pK_a of 6.5, possibly a histidine residue (Ribeiro et al., 1993). Functionally, NO is thought to bind tightly to nitrophorins at the low pH of *R. prolixus* saliva but is quickly released upon injection of saliva into the host, where it induces local vasodilation. Interestingly, nitrophorins also facilitate blood feeding by functioning as anticlotting factors (nitrophorin II only) and antihistamines. The anticlotting activity is independent of the heme moiety (Ribeiro et al., 1995; Sun et al., 1996), and the antihistamine activity is due to coordination of histamine with the heme iron (Ribeiro & Walker, 1994).

Other ferric heme proteins (e.g., metmyoglobin and methemoglobin) can bind nitric oxide, but the NO−heme complex undergoes autoreduction to the ferrous state, where nitric oxide binding is essentially irreversible (Addison & Stephanos, 1986). Nitrophorins can apparently bind and release NO without ever being reduced to the ferrous form (Ribeiro et al., 1993). This difference in reduction by NO is probably related to function: globins transport or store oxygen using ferrous heme, while nitrophorins transport NO using ferric heme. It is not yet known if nitrophorins stabilize the ferric form of heme through a diminished redox potential relative to globins or by some other mechanism.

† This work was supported in part by National Institutes of Health Grants A135591 (D.E.C.), HL54826 (W.R.M. and J.M.C.R.), and T32 CA09213 (J.F.A.) and Arizona Disease Control Research Commission Grant 9408 (W.R.M.).

* Corresponding author: Tel, (520) 621-1884; Fax, (520) 621-1697; E-mail, montfort@biosci.arizona.edu.

‡ Department of Biochemistry.

§ Department of Veternary Sciences. Present address: Department of Entomology, University of Georgia, Athens, GA 30602.

|| Department of Entomology.

⊗ Abstract published in *Advance ACS Abstracts,* April 1, 1997.

[1] Abbreviations: NO, nitric oxide; DTT, dithiothreitol.

S0006-2960(96)02888-7 CCC: $14.00

Nevertheless, the ability to reversibly bind NO is crucial to the physiological function of nitrophorins as vasodilators (Ribeiro et al., 1993).

The purification of large quantities of nitrophorins from *R. prolixus* salivary glands is difficult due to the extremely small size of the glands. Each gland has to be surgically removed and contains only microgram quantities of the proteins. Isolation of the individual nitrophorins is further hampered by their high similarity. In this study we report the expression and purification of milligram quantities of nitrophorin I and the rate and equilibrium binding constants for NO dissociation from the protein at several pHs. In addition, we describe crystals of the protein suitable for high-resolution X-ray diffraction studies.

MATERIALS AND METHODS

Plasmid Construction. The cDNA for nitrophorin I was modified for insertion into the expression vector pET17b by PCR mutagenesis. An *Nde*I restriction site and ATG start codon were created immediately 5′ of the codon for the N-terminal lysine residue in the native protein, as previously determined by Edman degradation. The portion of the open reading frame removed in this operation encodes the putative signal sequence for secretion to the salivary gland lumen. Mutagenesis of the nitrophorin I cDNA in pBluescript II was accomplished using the oligonucleotide CGCTCGAGCATATGAAGTGTACAAAAAATGCACTAGC in a PCR reaction along with the T7 sequencing primer TAATACGACTCACTATAGGGAGA as the reverse primer. The PCR product was ligated into the plasmid pCR2 using the protocols provided with the TA cloning kit (Invitrogen). After verification of the insert sequence the cloned PCR product was cut with *Nde*I and *Xho*I, and the fragment was inserted into pET17b (Novagen) to give the plasmid pET17B-NP1. *Escherichia coli* (INVαF′) cells were transformed with the ligation mixture. The plasmid was then moved into *E. coli* (BL21DE3) to give the expression strain *E. coli* (pET17B-NP1).

Expression of Nitrophorin I in E. coli. Nitrophorin I was isolated from insoluble inclusion bodies using the following protocol. Six liters of Luria broth (with 100 μg/mL ampicillin) in six 2 L Fernbach flasks was inoculated with an overnight culture of *E. coli* (pET17B-NP1). The flasks were shaken at 37 °C and 150 rpm until the OD_{600} of the cultures was approximately 0.6. IPTG was added to a concentration of 0.4 mM, and the cultures were shaken at 30 °C for 15−18 h at 150 rpm. The cells were harvested by centrifugation, washed with 50 mM NaH_2PO_4, pH 7.4, and stored at −70 °C. For lysis, cells were suspended in 100 mM Tris-HCl, pH 7.4, 20 mM EDTA, 10% sucrose, and 200 μg/mL lysozyme (buffer A). After incubation with stirring for 60 min at room temperature, the spheroplasts were collected by centrifugation at 20000*g* for 35 min. Lysis was accomplished with a French press (16 000−18 000 psi), and the lysate was incubated with a mixture of DNase I and RNase A (50 μg/mL each) for 60 min. The cell lysate was centrifuged at 20 000*g* for 30 min, and the pellet was suspended in 30 mM Tris-HCl, pH 7.4, 30 mM NaCl, 1 mM EDTA, and 1% (w/v) Triton X-100 (buffer B). The insoluble material was collected by centrifugation at 20 000*g* and washed two more times with Triton X-100-containing buffer B and two times in buffer B without Triton-X100.

Inclusion bodies were solubilized in 20 mL of 30 mM Tris-HCl, pH 7.4, 1 mM EDTA, 6 M guanidine hydrochloide, and 5 mM DTT (buffer C). After centrifugation at 100000*g* for 40 min, the denatured protein was refolded by dropwise addition over a period of 80 min to a 50-fold larger volume of 30 mM Tris-HCl, pH 7.4, 0.8 M NaCl, 1 mM EDTA, 10 mM DTT, and 15 mM PMSF (buffer D) at 0 °C. The diluted protein was stirred overnight at 4 °C. After centrifugation, the protein solution was concentrated by ultrafiltration through a 10 kDa MCO membrane (Amicon). The concentrated protein (75 mL) was dialyzed against two changes of buffer (100 mM NaH_2PO_4, pH 7.0), and a solution containing 10 mM hemin in DMSO was slowly added to the mixture while being stirred. Full incorporation of heme required repeated additions of hemin followed by removal of precipitated excess hemin through centrifugation (100000*g* for 30 min). The incorporation of heme was monitored using the ratio of the Soret absorbance at 404 nm to the absorbance at 280. A ratio of approximately 3.0 despite continued addition of hemin indicated full titration of the refolded protein to its native state.

The pH of the refolded heme protein solution was adjusted to 5.0 with 1 M acetic acid, and the solution was centrifuged at 100000*g*. The supernatant was applied to a 50 mL SP-Sepharose column equilibrated at room temperature with 25 mM sodium acetate, pH 5.0 (buffer E), the column was washed, and nitrophorin I was eluted using a gradient of 0−1 M NaCl in buffer E. Fractions containing nitrophorin I (based on absorbance spectra) were pooled, dialyzed, and concentrated.

Nitrophorin I was also purified from the salivary glands of *R. prolixus* using a combination of chromatofocusing and cation-exchange chromatography as described previously (Champagne et al., 1995).

Spectral Measurements and Nitric Oxide Binding. Optical spectra were measured on a Perkin-Elmer lambda-19 spectrophotometer at 25 °C in either 20 mM sodium acetate, pH 5.0, or 20 mM sodium phosphate, pH 7.3. Nitric oxide-saturated water (1.9 mM; Butler & Williams, 1993) was prepared by purging a sealed tube containing distilled water with argon for at least 30 min followed by bubbling NO into the water for a period of approximately 5 min. Protein samples were prepared in sealed 50 μL or 0.5 mL cuvettes and purged with argon for at least 30 min. NO-saturated water was added to the cuvette with a syringe, and the binding was measured by quantification of the shift in the Soret absorbance from 404 nm to a position near 420 nm in the visible spectrum.

The concentration dependence of NO binding was measured from NO-ligated minus unligated difference spectra. Small aliquots of NO-saturated water were added to protein solutions in sealed 0.5 mL cuvettes that were filled to near completeness and purged with argon. The total addition of NO-saturated water did not in any case exceed 5% of the initial volume of the sample.

All nitrophorin I concentrations were determined using an extinction coefficient of 169 mM^{-1} cm^{-1} for the Soret maximum of oxidized, unligated protein as reported previously (Champagne et al., 1995).

Kinetics of Nitrophorin Release. The kinetics of nitric oxide release from nitrophorin I were studied at 25 °C, pH 8.3, by stopped-flow spectrophotometry. Either insect-derived or recombinant nitrophorin I (1.2 μM in 10 mM sodium acetate, pH 5.0, 100 mM NaCl) was purged with argon and loaded with nitric oxide by adding NO-saturated water (1.9 mM) to a concentration of 10 μM. One syringe

on the stopped-flow device was filled with this solution and the other with 100 mM Tris-HCl, pH 8.3. After mixing, the increase in absorbance at 404 nm was monitored.

The kinetics of release at pH 5.0 were also determined. One hundred microliters of a 20.5 μM solution of nitrophorin I in 100 mM sodium acetate, pH 5.0, was placed in a 1.0 mL cuvette, which was sealed and purged with argon. Nitric oxide was added as 1.0 μL of a saturated aqueous solution to a final concentration of 19 μM. The solution was mixed and diluted by addition of 1.0 mL of 100 mM sodium acetate, pH 5.0, that had been purged with argon. The release of nitric oxide was measured by monitoring the change in absorbance at 404 nm in a Shimadzu UV160U spectrophotometer at 25 °C.

Crystallization of Nitrophorin I. Crystallization experiments with both insect-derived and recombinant proteins have been performed. The hanging-drop vapor-diffusion (McPherson, 1990) and sparse-matrix (Jancarik & Kim, 1991) approaches were used to obtain hexagonal rod-shaped crystals of the insect-derived protein at room temperature from a 1.7 mg/mL protein stock, pH 6.5−7.0, with poly(ethylene glycol) 4000 and 5% isopropyl alcohol as precipitating agents.

The purified recombinant protein was concentrated by ultrafiltration through a 10 kDa MCO Amicon filter to 20 mg/mL in 10 mM potassium phosphate buffer, pH 7.0. Two crystal forms of the recombinant protein have been obtained at room temperature, and their crystallization conditions were refined to (1) 0.2 M sodium acetate, 0.1 M sodium cacodylate, pH 6.5, and 25% PEG 8000 (thin needles) and (2) 2.6 M ammonium phosphate and 0.1 M potassium cacodylate, pH 5.3 (plate form). Large crystals of the plate form grew after small crystals were seeded into 5 μL drops composed of equal volumes of protein solution and precipitant solution (2.6 M ammonium phosphate, 0.1 M potassium cacodylate, pH 5.3), followed by an increase in the ammonium phosphate concentration over 6 days to 3.0 M.

A single 0.6 × 0.6 × 0.06 mm crystal of the plate form was used for data collection to 1.8 Å at room temperature. Diffraction data were measured using an Enraf Nonius FAST area detector attached to an FR571 rotating Cu anode with a graphite monochromator. Data reduction was performed using the software packages MADNES (Messerschmidt & Pflugrath, 1987) and PROCOR (Kabsch, 1988). Reflections were scaled with Rotavata/Agrovata programs (Collaborative Computational Project, 1994). Patterson self-rotation functions were calculated using X-PLOR (Brunger, 1987).

RESULTS AND DISCUSSION

Expression and Purification of Nitrophorin I. A modified cDNA for nitrophorin I, in which the sequence encoding the 23-residue signal peptide of the protein (Champagne et al., 1995) had been removed using PCR mutagenesis, was cloned into the expression vector pET17b and transformed into *E. coli* strain pET17B-NP1. Induction of T7 polymerase expression resulted in the production of a polypeptide which had a molecular mass of 20 500 Da and comigrated on SDS−PAGE with an authentic sample of nitrophorin I isolated from the salivary glands of *R. prolixus*.

Nitrophorin I could be obtained only in the insoluble fraction of the cell lysate as inclusion bodies, despite numerous alterations in growth conditions. Inclusion body preparations were, however, successfully renatured, and heme

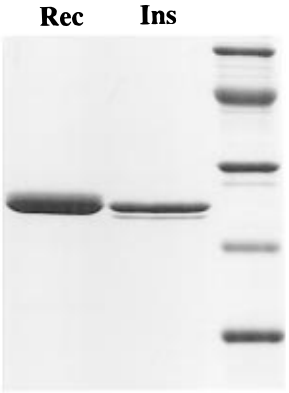

FIGURE 1: Comparison of recombinant and insect-derived nitrophorin I by SDS−polyacrylamide gel electrophoresis. Rec = purified renatured recombinant nitrophorin I; Ins = nitrophorin I partially purified from *R. prolixus* salivary glands. Standards: α-lactalbumin, soybean trypsin inhibitor, carbonic anhydrase, ovalbumin, and bovine serum albumin.

was incorporated to give native protein as indicated by the UV−visible spectrum. The renaturation protocol was based on that of Matsushima et al. (1994) in which the protein was completely dissolved in concentrated guanidine and refolded by dilution into a buffer containing high concentrations of sodium chloride and the reductant DTT. DTT was required during refolding, presumably to prohibit the formation of incorrect disulfide bonds. The success of renaturation was apparent when a solution of hemin in DMSO was added to a dilute solution of refolded protein. Successive additions of hemin led to a concomitant increase in the absorbance of the Soret band characteristic of native nitrophorin I (404 nm). Saturation of the heme binding pocket was indicated by a lack of increase in A_{404} with successive additions of hemin. The reconstituted protein was purified to homogeneity by cation-exchange chromatography (Figure 1), resulting in an overall yield from the entire procedure of 30−50 mg of purified protein/L of culture. Edman degradation of the purified recombinant protein gave the sequence MKCTK, indicating the addition of an initiator methionine residue to the N-terminus of the insect-derived protein. Characterization of the reconstituted protein (see below) showed that the properties of the recombinant material were virtually identical to those of insect-derived nitrophorin I and that the presence of an additional methionine residue at the N-terminus of the protein had no detectable effect on its function as a nitric oxide carrier.

Optical Properties of Nitrophorin I. The optical spectrum of the purified, renatured material in pH 7.0 phosphate and pH 5.0 acetate showed a Soret maximum at 404 nm and a ratio of the Soret band to the 280 nm absorbance of 3.1 (Figure 2A). The position of the Soret maximum was identical to the insect-derived protein, and the A_{404}/A_{280} ratio indicated that the protein was comparable to the insect-derived protein in purity and degree of saturation with heme (Figure 2). When nitric oxide was added to the protein under anaerobic conditions, the Soret maximum shifted to 419 nm at pH 7.0 (Figure 2) and 421 nm at pH 5.0 (Figure 3), indicating the formation of a nitrosylheme complex. Nitrosation also resulted in the appearance of prominent α and β bands at 569 and 533 nm in both high and low pH spectra (Figure 2). At pH 7.0, purging of the nitrosyl heme protein solution with argon for 15 min resulted in a return of the Soret maximum to 404 nm and a loss of the prominent α and β bands. At pH 5.0, however, the position of the Soret

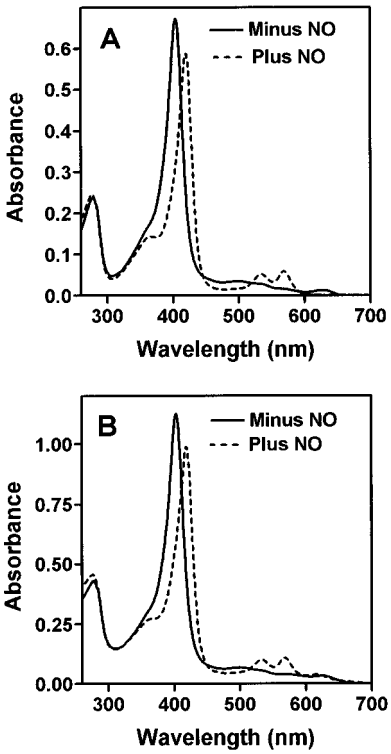

FIGURE 2: Absolute absorption spectra of unligated (—) and NO-ligated (- - -) nitrophorin I in sodium phosphate, pH 7: (A) recombinant protein; (B) insect-derived protein.

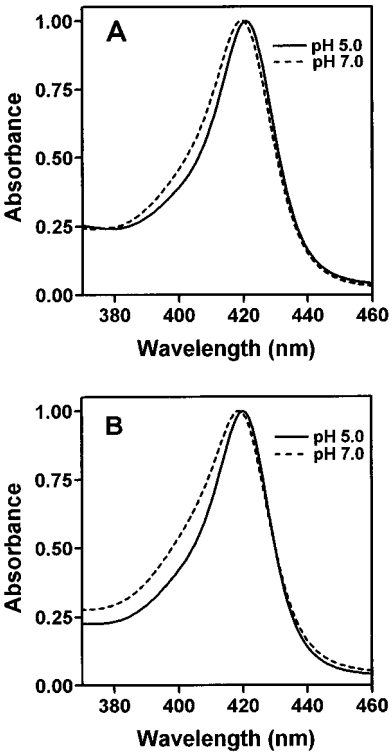

FIGURE 3: Normalized spectra of the Soret region of NO-bound nitrophorin I in sodium phosphate, pH 7.0 (- - -), and sodium acetate, pH 5.0 (—): (A) recombinant protein; (B) insect-derived protein.

maximum did not completely revert to 404 nm on purging with argon, indicating that nitric oxide had not completely dissociated from the protein (data not shown). The reversible binding of NO to a mixture of ferric nitrophorins at pH 7.0 and the apparent increase in affinity at pH 5.0 have been previously described (Ribeiro et al., 1993). Direct comparison of spectra obtained from the recombinant protein with those of the insect-derived protein shows the two proteins to be essentially indistinguishable (Figures 2 and 3).

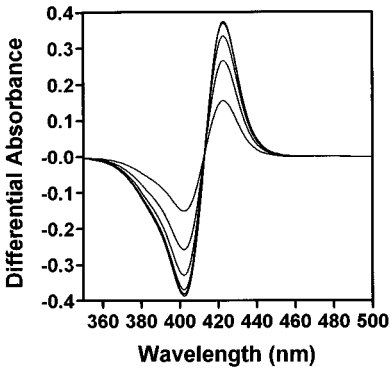

FIGURE 4: Difference spectra (NO-ligated minus unligated) for recombinant nitrophorin I in sodium phosphate, pH 6.0. NO concentrations are 12, 24, 36, 48, 60, and 72 μM.

Table 1: pH Dependence of Spectral Properties for Recombinant Nitrophorin I[a]

pH[b]	maximum[c]	minimum[d]	D_{max}[e]
5.0	423	402	0.76
6.0	423	402	0.76
6.5	423	402	0.77
7.0	422	402	0.66
7.3	422	402	0.68

[a] All experiments done at a nitrophorin I concentration of 4.7 μM. [b] pH 5.0, 10 mM sodium acetate; pH 6.0, 10 mM sodium acetate; pH 6.5, 10 mM sodium phosphate; pH 7.0, 10 mM sodium phosphate; pH 7.3, 10 mM sodium phosphate. [c] Absorbance maximum (nm) in the NO-ligated minus unligated difference spectrum (Figure 4). [d] Absorbance minimum (nm) in the NO-ligated minus unligated difference spectrum (Figure 4). [e] Maximum value of (A_{423} or A_{422}) − A_{402}.

The pH-dependent changes in the nitrophorin spectra were quantified by subtracting the spectra of the fully ligated protein from that of the unligated protein for a series of pHs. Figure 4 shows the difference spectra at pH 6.0 for increasing concentrations of NO, and Table 1 lists the maximal difference in spectra obtained at several pHs. Two major pH-dependent features of the nitrophorin spectra were observed: a bathochromic shift in the position of the spectral maximum (as described above) and a decrease in the magnitude of the maximal change in the difference spectra (Table 1). At pH 5.0, 6.0, and 6.5 the difference spectra were nearly identical. However, at pH 7.0 and 7.3 the position of the maxima shifted by 1 nm and the maximal change in the difference spectra decreased by ∼12% with respect to the values at lower pH (Table 1). These shifts in the absorption spectra are likely to reflect a functional change in the protein, since binding of NO varies with a similar pH dependency, both for recombinant nitrophorin I (shown below) and for salivary gland extracts containing nitrophorins I−IV (Ribeiro et al., 1993).

Binding Studies. Difference spectra were also used to quantify the binding of NO to recombinant nitrophorin I at several pHs. Increasing amounts of NO were added to an anaerobic solution of nitrophorin I under conditions where the protein concentration was less than or equal to the lowest NO concentration, resulting in a series of difference spectra similar to those in Figure 4 for each pH studied. Plots of NO concentration vs the proportion of the maximum spectral change displayed typical saturation behavior (not shown), allowing for dissociation constants to be determined from nonlinear regression analyses of the plots. The resulting K_d

Table 2: Nitric Oxide Dissociation Constants of Ferric Nitrophorin I at Three pH Values

pH	K_d (μM ± SE)[a]
5.0[b]	0.19 ± 0.02
6.0	0.62 ± 0.06
8.3	1.71 ± 0.17

[a] Calculated by fitting a rectangular hyperbolic function using the program Enzfitter (Biosoft, Ferguson, MO). [b] pH 5.0 experiment performed in 20 mM sodium acetate, pH 6.0 in 20 mM sodium citrate, and pH 8.3 in 20 mM Tris-HCl.

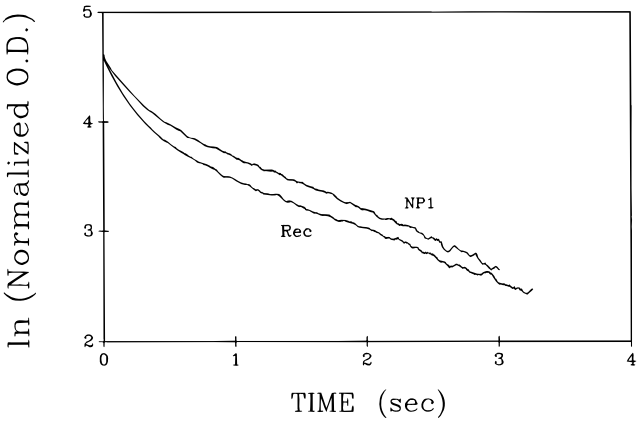

FIGURE 5: Kinetics of NO dissociation from nitrophorin I after simultaneous 2-fold dilution and increase in pH from 5.0 to 8.3. Rec = recombinant protein; NP1 = nitrophorin I isolated from *R. prolixus* salivary glands.

at pH 5.0 is submicromolar and increases approximately 9-fold at pH 8.3 (Table 2).

The dissociation constants measured for nitrophorin I are 2−3 orders of magnitude lower than those of ferric heme proteins such as sperm whale myoglobin ($K_d = 2.6 \times 10^{-4}$ M) but are similar to the value obtained with elephant myoglobin (1.8×10^{-6} M) (Sharma et al., 1987; Hoshino et al., 1993). The enhanced binding of NO to ferric elephant myoglobin has been attributed to the absence of a coordinated water molecule in the distal heme position, since, if present, such a water molecule must first be dislodged before NO can bind (Sharma et al., 1987). Axially bound water is stabilized in sperm whale myoglobin by a distal histidine that is absent in elephant myoglobin (Sharma et al., 1987). That nitrophorin may also lack a distal histidine is suggested by both its tight binding to NO and its apparent pentacoordinate high-spin Fe(III) heme (Ribeiro et al., 1993).

Kinetic Studies. The dissociation rate of NO from recombinant and insect-derived nitrophorin I was determined at pH 8.3 by monitoring the spectral changes that occur upon NO release. To obtain these rates, the protein was first loaded with NO at pH 5.0, where binding is more stable, and then rapidly diluted into a pH 8.3 solution using a stopped-flow device. NO release was then monitored at 404 nm. Both the insect-derived and recombinant nitrophorin I displayed a biphasic increase in A_{404} (Figure 5), indicating the presence of two first-order dissociation rate constants that differ by ~10-fold (listed as "fast" and "slow" in Table 3; the fast dissociation accounted for approximately 90% of the observed spectral change). The fast-phase NO release rate constants are slightly slower than those for ferric whale and elephant myoglobins, which are 14 and 40 s^{-1}, respectively (Sharma et al., 1987).

The release rate for NO at pH 5.0 was also measured for the recombinant protein by dilution under anaerobic conditions (data not shown). As expected, the first-order release rate was considerably slower at pH 5.0, down approximately 2500-fold from the fast dissociation rate at pH 8.3 (Table 3). Previous experiments undertaken with whole gland extracts have shown that purging with argon at low pH does not fully restore the protein to the unligated condition within 15−30 min (Ribeiro et al., 1993).

Table 3: First-Order Rate Constants (s^{-1}) for Nitric Oxide Dissociation from Nitrophorin I

	insect-derived[a]	recombinant[b]
pH 8.3		
fast	3.9 ± 0.3[c]	3.0 ± 0.2[c]
slow	0.35 ± 0.02[c]	0.27 ± 0.02[c]
pH 5.0	nd[d]	$(1.21 \pm 0.09) \times 10^{-3}$ [e]

[a] Purified from *R. prolixus* salivary glands. [b] Purified from *E. coli* (pET17b-NP1) extracts. [c] Average of 8−10 replicates (±SE). The fast phase accounted for approximately 90% of the change in absorbance. [d] Not determined. [e] Average of three replicates (±SE).

It is interesting that the dissociation rate at pH 5.0 was monophasic, while upon rapid dilution into a pH 8.3 solution, two release rates were observed. A possible explanation for the biphasic kinetics would be the involvement of a second binding group for NO on the protein at higher pHs that could deliver NO to the heme. The possible involvement of nonheme functional groups in NO binding to a heme protein has been recently described for ferrous guanylate cyclase (Stone & Marletta, 1996) and hemoglobin (Jia et al., 1996). Additional experiments are required to resolve this issue.

With the K_d and dissociation rate constants known, the rate constant for association of NO with nitrophorin I can be calculated. The value of 2×10^6 M^{-1} s^{-1} found for nitrophorin I at pH 8.3 (using the fast dissociation rate) is closer to that for ferric elephant myoglobin (2×10^7 M^{-1} s^{-1}) than for ferric sperm whale myoglobin (5×10^4 M^{-1} s^{-1}) (Sharma et al., 1987). As discussed above, a faster association rate is consistent with the presence of a single axial histidine residue since no displacement of a bound water molecule is involved in the binding mechanism. It should be noted that these comparisons are complicated by the tendency for NO to autoreduce ferric myoglobin to the ferrous form. However, the autoreduction rate [2.17×10^{-4} s^{-1} for NO-bound ferric myoglobin at 1 atm of NO (Addison & Stephanos, 1986)] is quite slow relative to the NO association rate, making it possible to directly compare the NO association rates for the two proteins.

At pH 5.0, the first-order rate constant for NO release by nitrophorin I is reduced 3 orders of magnitude while the dissociation constant is reduced only 10-fold. Therefore, the value obtained for the association rate constant (6.4×10^3 M^{-1} s^{-1}) is 100 times lower than at pH 8.3 and even slower than that for sperm whale myoglobin. Thus, both binding and release of NO to nitrophorin I are apparently hindered under acidic conditions, possibly due to a pH-dependent conformational change in the protein.

Crystallization of Nitrophorin I. Three crystal forms of nitrophorin I have been obtained: (1) hexagonal rod-shaped crystals of the insect-derived protein, (2) needle-shaped crystals of the recombinant protein, and (3) a monoclinic plate form of the recombinant protein. A hexagonal rod-shaped crystal measuring approximately 0.1 × 0.1 × 0.05 mm diffracted to 3 Å and displayed unit cell parameters of $a = b = 80.1$ Å, $c = 64.0$ Å, $\alpha = \beta = 90.0°$, and $\gamma = 120.0°$. These parameters are consistent with a hexagonal

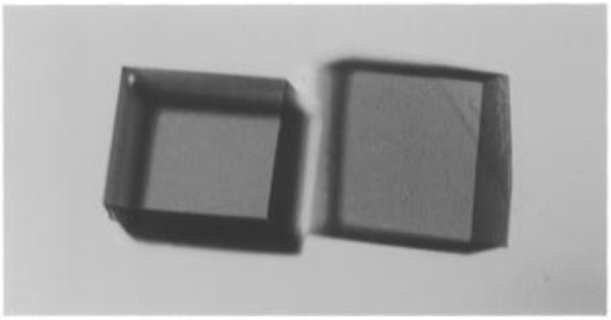

FIGURE 6: Monoclinic crystals of nitrophorin I. The largest dimension is about 1 mm.

space group containing one molecule of protein per asymmetric unit (molecular mass 20 378 Da) and a solvent content of about 50% (Matthews, 1968). The monoclinic crystals grow to 1 mm across, diffract beyond 1.8 Å nominal resolution, and belong to the monoclinic space group $P2_1$ with cell dimensions $a = 39.5$ Å, $b = 74.2$ Å, $c = 66.3$ Å, and $\beta = 99.5°$. These parameters are consistent with two protein molecules and 48% solvent in the asymmetric unit. At present, only the monoclinic crystal form is being pursued.

Unfortunately, most of the monoclinic crystals are internally twinned in a manner that is difficult to detect visually but clearly apparent in the diffraction pattern. We have been able to reduce the number of twinned crystals we obtain and increase the thickness of the plates using the following unconventional technique. Small crystals growing with the plate plane (*bc* plane) parallel to the drop surface are transferred to a new hanging drop, oriented with the plate plane parallel to the drop surface, and equilibrated against 2.6 M ammonium phosphate. At this precipitant concentration, the transferred crystals grow but nucleation of new crystals does not occur. After 2 days, the ammonium phosphate concentration of the well buffer is increased to 2.8 M, and after an additional 2 days to 3.0 M, where the crystals are more stable to minor temperature fluctuations. The resulting crystals are thicker and display less twinning, suggesting that fast growth along the plate plane contributes to the twinning phenomena. These crystals can be grown in the unusually wide pH range of 5.3−8.3. A nitrophorin crystal is shown in Figure 6.

We have located a noncrystallographic 2-fold symmetry axis relating the two protein molecules in the crystal asymmetric unit. A distinct peak at $\psi = 90.0°$ and $\phi = 22.5°$ was found in the $\kappa = 180°$ section of a Patterson self-rotation function map calculated with amplitudes between 8.0 and 4.0 Å resolution. No other peaks above background were observed. This peak is consistent with the existence of a 2-fold symmetry axis oriented parallel to the *ac* plane and inclined at 22.5° to the *ab* plane.

We have noticed that nitrophorin I changes to a deep red color in the presence of NH_4^+, which is used as a precipitant for crystallization (Figure 6). This change in color can be reversed by transferring crystals to 2.5 M potassium phosphate. A shift in the Soret absorption maxima also occurs in the presence of ammonium phosphate, from 404 to 410 nm. These observations suggest that an NH_3 ligand can bind reversibly to the heme group of nitrophorin I.

Finally, the four cysteines in the protein appear to form two disulfide bonds, as mercuric compounds do not react with the crystals. The occurrence of these disulfide bonds is most likely the reason reductant is required for successful renaturation of the recombinant protein.

Conclusions. Studies on the novel nitric oxide binding protein nitrophorin I have been hampered by the difficulty in obtaining large amounts of *R. prolixus* salivary gland tissue as a source of the protein. The development of a heterologous expression system has allowed the initiation of detailed structural and mechanistic studies designed to elucidate the means by which nitrophorin I is able to function as a NO transport protein while other heme proteins are poisoned by the gas. Toward this end, we have presented here detailed information concerning binding of NO by nitrophorin I, the effect of pH on this binding, and crystals that should lead to a high-resolution structure of the protein.

ACKNOWLEDGMENT

The authors thank Prof. Ann Walker and Dr. Terry Meyer for critical reading of the manuscript, as well as Prof. René Feyereisen for the use of the lambda-19 spectrophotometer.

REFERENCES

Addison, A. W., & Stephanos, J. J. (1986) *Biochemistry 25*, 4104−4113.
Bredt, D. S., & Snyder, S. H. (1994) *Annu. Rev. Biochem. 63*, 175−195.
Brunger, A. T., Kuriyan, J., & Karplus, M. (1987) *Science 235*, 458−460.
Butler, A. R., & Williams, D. L. H. (1993) *Chem. Soc. Rev.*, 233−241.
Champagne, D. E., Nussenzvieg, R. H., & Ribeiro, J. M. C. (1995)- *J. Biol. Chem. 270*, 8691−8695.
Collaborative Computational Project, No. 4 (1994) *Acta Crystallogr. D50*, 760−763.
Jancarik, J., & Kim, S.-H. (1991) *J. Appl. Crystallogr. 24*, 409−411.
Jia, L., Bonaventura, J., & Stamler, J. S. (1996) *Nature 380*, 221−226.
Kabsch, W. (1988) *J. Appl. Crystallogr. 21*, 916−934.
Matsushima, S., Huang, Y.-P., Dudas, C., Guerriero, V., & Hartshorne, D. J. (1994) *Biochem. Biophys. Res. Commun. 202*, 1329−1336.
Matthews, B. W. (1968) *J. Mol. Biol. 33*, 491.
McPherson, A. (1990) *Eur. J. Biochem. 189*, 1−23.
Messerschmidt, A., & Pflugrath, J. W. (1987) *J. Appl. Crystallogr. 20*, 306−315.
Ribeiro, J. M. C., & Walker, F. A. (1994) *J. Exp. Med. 180*, 2251−2257.
Ribeiro, J. M. C., Hazzard, J. M. H., Nussenzveig, R. H., Champagne, D. E., & Walker, F. A. (1993) *Science 260*, 539−541.
Ribeiro, J. M. C., Schneider, M., & Guimaraes, J. A. (1995) *Biochem. J. 308*, 243−249.
Schmidt, H. H. H. W., & Walter, U. (1994) *Cell 78*, 919−925.
Sharma, V. S., Traylor, T. G., & Gardiner, R. (1987) *Biochemistry 26*, 3837−3843.
Stone, J. R., & Marletta, M. A. (1996) *Biochemistry 35*, 1093−1099.
Sun, J., Yamaguchi, M., Yuda, M., Miura, K., Takeya, H., Hirai, M., Matsuoka, H., Ando, K., Watanabe, T., Suzuki, K., & Chinzei, Y. (1996) *Thromb. Hemostasis 75*, 573−577.
Traylor, T. G., & Sharma, V. S. (1992) *Biochemistry 31*, 2847−2849.
Tsai, A.-L. (1994) *FEBS Lett. 341*, 141−145.
Valenzuela, J. G., Walker, F. A., & Ribeiro, J. M. C. (1995) *J. Exp. Biol. 198*, 1519−1526.

BI9628883